SLAC-PUB-1420
ITP-465
(T/E)
May 1974

EXPERIMENTAL CONSEQUENCES OF QUARK-STRUCTURE *

Geoffrey B. West
Institute for Theoretical Physics, Dept. of Physics
Stanford University, Stanford, Calif. 94305

Peter Zerwas**
Stanford Linear Accelerator Center
Stanford University, Stanford, Calif. 94305

(Submitted to Phys. Rev.)

*Work supported in part by the U.S. Atomic Energy Commission and by the National Science Foundation.

**Max Kade Fellow; on leave of absence from Tech. Hochschule Aachen, W. Germany.

ABSTRACT

Some experimental consequences of endowing quarks with both a finite size (form factor) as well as an anomolous magnetic moment are investigated within the context of the naive quark-parton model. Our discussion is limited to experiments which will be completed in the near future such as deep inelastic electroproduction at large angles and high energies, electron-positron colliding beam experiments, high energy neutrino and antineutrino scattering and the production of μ pairs. The following are some definite predictions of the model which can be tested: (a) the ratio of longitudinal to transverse cross-sections must begin to rise beyond $-q^2 \sim 10(\text{GeV}/c)^2$ reflecting a considerable scaling violation in the conventional W_1 structure function; (b) the normalized single particle distribution functions $(1/\sigma)(d\sigma/dz)$ (z being the fractional energy carried off by the detected particle) should scale in both ep and e^+e^- processes; (c) the approach to scaling in these distributions should be much slower for smaller values of z; (d) in e^+e^-, the single particle distribution function $s(d\sigma/dz)$ should violate scaling, especially for smaller values of z; (e) there should be only small deviations, if any, from scaling in antineutrino scattering whereas deviations in neutrino scattering should be considerable. Finally, similar experimental consequences of the presence of a second class current in the weak interactions are explored.

I. INTRODUCTION

Deep inelastic lepton scattering experiments have proven to be the most powerful means for investigating the substructure of nuclear matter. All of these experiments can be successfully described by assuming that the nucleon consists of a number of pointlike particles from which the leptons scatter incoherently.[1] Identifying these particles (often called partons) with quarks leads to a consistent picture of the electromagnetic as well as weak experiments provided one is willing to ignore the problem of quark confinement. This caveat has become an integral part of the quark model folklore where one treats the hadrons as "loosely" bound systems of quarks with a relatively small effective mass ($\sim$ 350 MeV). Chanowitz and Drell[2] (CD) have pointed out that, from a conservative viewpoint, the forces that bind the quarks together inevitably give the quarks a finite size, no matter how weak the effective binding. This is certainly the case in the nucleus where mesons not only keep the nucleons bound but also give them a finite size as well as an anomalous magnetic moment. The same effect also occurs in conventional quantum electrodynamics. Of course, quarks may not be--and, indeed, probably are not--conventional so it might be possible to define theories where they do not appear as asymptotic states and yet behave as if they are light constituents of the hadrons. They might, for instance, be purely fictitious, being only a shorthand for a complicated bootstrap scheme. In such cases it is feasible that a quark structure is not induced by the binding interactions. A great deal of theoretical attention has been given to these problems of late and the matter has become particularly interesting most recently because of the unexpected experimental result for the total cross-section[3] $\sigma(e^+e^- \rightarrow \text{all hadrons})$. Point-like quark models predict a $1/s$ asymptotic fall-off of the cross-section ($\sqrt{s}$ being the total centre of mass energy of the electron-positron system) whereas experiments reveal an approximately constant behavior. On the other hand, it has recently been shown[4] by one of us that structured quarks (i.e., quarks with a size and an anomalous magnetic moment) admit the possibility of a roughly constant total cross-section in the region where data have been taken. At the same time, reasonable parameters can be chosen so as to leave the observed scaling phenomenon in the deep inelastic region intact.

Insofar as the question of quark structure is of fundamental importance for the success of the physical quark parton model, we have undertaken in this article further detailed investigations of its consequences in various processes: e^+e^- annihilation experiments, neutrino scattering experiments and $\mu^+\mu^-$ pair production processes. Our motivation is to summarize some of the more salient consequences of quark structure which could feasibly be observed in the near future in experiments that are already underway. Hopefully these can help settle whether such an effect should be taken seriously. For instance, we shall show that the almost perfect cancellation of such effects in the electron scattering case is no longer possible in neutrino scattering where the kinematics are different due to the polarization of the leptons. The central physical assumption for handling deep inelastic scattering in the parton model is embodied in the impulse approximation. In our calculations we shall assume that such an assumption is not invalidated when the quarks are dressed. Chanowitz and Drell[2] have investigated this problem within the context of a quark-gluon model and have shown that at high enough energies (but still below the gluon production threshold) such an assumption can indeed be justified (at least in the absence of an anomolous magnetic moment). Intuitively this is certainly what one expects; for instance, in the scattering of high energy electrons from nuclei it is sufficient to treat the nucleus as a bound state of N nucleons, each of which is endowed with a form factor provided one remains below pion production threshold. In other words, we intuitively expect a short wave-length photon to be able to resolve the structure of individual quarks without being sensitive to the gluons being exchanged between them and which provide the binding. As in the conventional impulse approximation, the only effect of the binding is to provide a quark momentum distribution in the guise of a wave-function. Throughout most of this paper we shall adopt this assumption and work within the context of the naive (or "kindergarten") quark-parton model as enunciated, for instance, by Feynman and Bjorken and Paschos.[1] The consequences of this approach can be summarized briefly as follows: $\sigma(e^+e^- \to \text{all hadrons})$ is nearly constant within the present energy range whilst the conventional proton structure function F_2 can be made almost scale invariant.[4] On the other hand, the ratio σ_L/σ_T should begin to rise with q^2 reflecting a sizeable breakdown of scaling in the structure function W_1. We shall further show that the single particle distributions $\frac{1}{\sigma}\frac{d\sigma}{dz}$ (z being the Feynman parameter representing the fractional longitudinal momentum carried off by the detected particle) should still scale for large enough z in both e^+e^- and ep scattering experiments. Furthermore the particles should come out almost isotropically distributed. In antineutrino scattering, we in general predict only a small deviation from scaling, whereas in the neutrino case we expect large effects. By taking ratios of neutrino and antineutrino cross-sections, one can factor out the form factor effects (much the same happens in the ratio σ_L/σ_T) leaving only effects due to the anomalous moment. This might be particularly useful for distinguishing any possible effect due to the propagator of a massive weak intermediate vector boson. Parenthetically, we also discuss possible effects due to the presence of second class currents in the weak interactions. Finally, we say a few words about $\mu^+\mu^-$-pair production in pp collisions.

The rest of the paper is devoted to discussing these topics in some detail, repeating some of the material to be found in refs 2 and 4 for the sake of completeness and the reader's convenience.

II. CONSEQUENCE OF QUARK STRUCTURE

a) Deep Inelastic Electron-Nucleon Scattering

In this subsection we sketch the calculation of ref. 4 in order to define our notation and remind the reader of the essential features. We shall use the so-called naive parton model where one ignores both the transverse parton momentum as well as its effective mass when making dynamical calculations. In this model one works in an infinite momentum frame and ascribes a probability function for a quark to be carrying some fraction η of the total momentum, $f(\eta)$ say. The conventional structure functions are then obtained from a convolution of this probability with the probability for scattering from individual quarks.

For point-like quarks this latter probability is derived from the electromagnetic vertex $e_i \gamma_\nu$ where e_i is the charge of the ith quark. For a quark with structure, this vertex is replaced by

$$e_i \{\gamma_\nu - (p+p')_\nu \mu_Q\} G(q^2) + O(m_Q^2, \mu_Q m_Q) \qquad (1)$$

where we have made explicit the fact that the effective quark mass m_Q is to be neglected; we remind the reader that hadron spectroscopy suggests that $m_Q \sim 300$ MeV. Our notation is as follows: p and p' are the quark momenta before and after the collision with a virtual photon of the four-momentum q; μ_Q is the anomolous magnetic moment of the quark whose magnitude is estimated to be $\sim .1\ \mathrm{GeV}^{-1}$ if the correct nucleon magnetic moments are to be reproduced. (For this rough estimate, we ignore any difference between current and constituent quarks.) In that case, we note that $\mu_Q m_Q \sim .03$ which in general we shall neglect as indicated in eq. (1). Finally, for the sake of simplicity, we have taken the electric and magnetic form factors of the quark to be identical and have neglected SU(3) breaking on the quark level.

Without quark structure we would have for the conventional $W_2(\nu, q^2)$ structure function (ν is the electron energy loss)

$$W_2(\nu, q^2) = 2 \sum_i \int_0^1 d\eta\ \eta\ f_i(\eta)\ e_i^2 \delta((\eta P + q)^2 - m_Q^2) \qquad (2)$$

which leads to the scaling result:

$$\nu W_2(\nu,q^2) \to \mathscr{F}_2(x) = \sum_i e_i^2 x f_i(x) \tag{3}$$

where $x = -q^2/2\nu$. $\mathscr{F}_2(x)$, in fact, depends only upon the variable x. It is generally assumed that the corrections to this result are $O(m_Q^2/q^2)$ which is consistent with dropping m_Q^2 in the delta-function. A small value of m_Q is then consistent with the rapid approach to scaling observed in the experiments. Now, with the addition of quark structure we find that

$$\nu W_2(\nu,q^2) \to F_2(x,q^2) = G^2(q^2)(1 - \mu_Q^2 q^2) \ \mathscr{F}_2(x) + O(m_Q^2, \ \mu_Q m_Q) \tag{4}$$

A similar calculation can be performed for the other structure function $W_1(\nu,q^2)$ to give

$$W_1(\nu,q^2) \to F_1(x,q^2) = G^2(q^2) \frac{\mathscr{F}_2(x)}{2x} + O(m_Q^2, \ \mu_Q m_Q) \tag{5}$$

In the structureless case we, of course, have the usual Callan-Gross relationship

$$W_1(\nu,q^2) \to \mathscr{F}_1(x) = \mathscr{F}_2(x)/2x$$

which implies that the ratio $\sigma_L/\sigma_T \to 0$. Here, however, we find that

$$\sigma_L/\sigma_T \to -\mu_Q^2 q^2 \tag{6}$$

Before discussing this we would like to sound a word of caution concerning the approach to scaling. Let us suppose that in the structureless case

$$\nu W_2(\nu,q^2) \to \mathscr{F}_2(x) + \frac{m_Q^2}{q^2}\,\mathscr{G}_2(x) \tag{7}$$

and

$$W_1(\nu,q^2) \to \frac{\mathscr{F}_2(x)}{2x} + \frac{m_Q^2}{q^2}\,\mathscr{G}_1(x) \tag{8}$$

then in the case with structure we would have

$$F_2(x,q^2) = G^2(q^2)\{-\mu_Q^2q^2\ \ \mathscr{F}_2(x) + \mathscr{F}_2(x)-\mu_Q^2m_Q^2\ \ \mathscr{G}_2(x)\} + O(m_Q^2,\ \mu_Q m_Q) \tag{9}$$

In other words, there are small non-vanishing scaling terms introduced due to the approach to scaling; however, to be consistent one must, of course, ignore such terms since comparable terms have already been implicitly neglected and justify it by appealing to the apparent smallness of m_Q. However, when we come to eq. (6) for σ_L/σ_T we note that corrections to this involve terms like $4\mu_Q m_Q$, $4M^2\ \mu_Q^2x^2$ as well as terms $O(m_Q^2,\ \mu_Q m_Q)$. Thus, although $\mu_Q^2q^2$ is obviously dominant asymptotically it will not reveal itself until

$$-q^2 \gg \max\left\{\frac{4m_Q}{\mu_Q}\ ,\ 4x^2M^2\right\} \approx 10\ \mathrm{GeV}^2\ .$$

In fig. 1 we show a plot of $-\mu_Q^2q^2$ together with the various data points taken from experiment.[5] Because of the approach to scaling problem at these energies and the possibility of systematic errors, no definite inference can yet be drawn.

As emphasized in ref. 4, $G(q^2)$ and μ_Q^2 can be chosen so as to ensure that $F_2(x,q^2)$ remains approximately scale invariant in the region $-q^2 \lesssim 15\ \mathrm{GeV}^2$. For example, parameterizing

$$G(q^2) = 1/(1 - q^2/\Lambda^2)$$

and choosing $\mu_Q^2 \approx .02/\mathrm{GeV}^2$ and $\Lambda^2 \approx 100\ \mathrm{GeV}^2$ keeps F_2 scale invariant within the errors of the experiment. Furthermore, $\mu_Q^2 \approx .02/\mathrm{GeV}^2$ keeps σ_L/σ_T to only ~ 20% for $-q^2 = 10\ \mathrm{GeV}^2$. In principle, measuring σ_L/σ_T provides the cleanest feasible method for detecting the presence of an anomolous magnetic moment. Experimentally one should see a relatively large violation of scaling in W_1 at $-q^2 \approx 30\ \mathrm{GeV}^2$ (~ 20-30%, say) while νW_2 should remain relatively unaffected. Present experiments at SLAC and NAL should directly confront this prediction.

b) e^+e^- Annihilation into Hadrons

In the naive quark-parton model this process is seen as basically measuring the probability for producing quark-antiquark pairs which decay into the real observed hadrons. As in deep inelastic scattering this final state interaction is ignored in the calculation. It is conventional to express the result in terms of the ratio $R = \sigma(e^+e^- \to \text{hadrons})/\sigma(e^+e^- \to \mu^+\mu^-)$; in the unstructured case this ratio is simply $\Sigma\, e_i^2$; i.e., a constant independent of s. With structure this result is amended to read:

$$R = \sum_i e_i^2 \frac{(1 + \frac{1}{2}\mu_Q^2 s)}{(1 - s/\Lambda^2)^2} + O(m_Q^2,\ \mu_Q m_Q) \tag{10}$$

which leads to an initial growth of R with s, in agreement with experiment. Indeed, with the choice of parameters mentioned above (i.e., $(\mu_Q^2 \sim .02\ \mathrm{GeV}^{-2}, \Lambda \sim 10\ \mathrm{GeV})$) this can be made to fit the data quite nicely.

Our main emphasis in this subsection is to investigate the implications of the model for the one-particle distribution functions. This is obtained by multiplying the probability for producing a quark-antiquark pair by the probability that the produced quark fragments into the given detected particle (a pion say). This latter probability is denoted[1] by D_i^π. In the ideal case of infinite energy, this model leads to:

$$\frac{1}{\sigma_\mu} \frac{d\sigma^\pi}{dz\ d\cos\theta} = \frac{3}{8} G^2(s)[(1 + \cos^2\theta) + \mu_Q^2 s(1 - \cos^2\theta)] \sum_i e_i^2 D_i^\pi(z) \qquad (11)$$

where z is the fraction of the pion energy relative to the beam energy, θ the angle between the outgoing pion and the beam axis and σ_μ the total μ-pair production cross-section. The reader is again reminded that terms of order $O(m_Q^2, \mu_Q m_Q)$ have been dropped here: we shall comment on this below. First let us comment on the consequences of this equation as it stands. Integrating over θ we find that:

$$f^\pi(z) = \frac{1}{\sigma(s)} \frac{d\sigma^\pi}{dz} = \frac{\Sigma\, e_i^2\, D_i^\pi(z)}{\Sigma\, e_i^2} \qquad (12)$$

is independent of s, i.e., it scales. In order to get some feeling for this, it is interesting to make a qualitative comparison with the analogous distribution in electroproduction. For $x \gtrsim .2$, say, i.e., well away from the diffractive region, we expect the nucleon to look most like a conventional bound state consisting predominantly of 2 up-quarks (u) and 1 down-quark (d). If these quarks have roughly equal distribution functions, i.e., $u(\eta) \approx 2d(\eta)$, then in this region

$$\frac{1}{\sigma}\frac{d\sigma^{\pi+}}{dz} \approx \frac{8}{9} D_u^{\pi+}(z) + \frac{1}{9} D_d^{\pi+}(z) \ . \tag{13}$$

We have here assumed the conventional quark charge assignments and have calculated the process in the spirit of eq. (2), i.e., a massive virtual photon strikes a parton which decays into a detected pion plus anything else, the latter being governed by the D_i^{π}. For small z (maybe even $z \lesssim 1/2$) we expect all the quark fragmentation functions to be roughly equal. In that case eq. (12) reduces to

$$f^{\pi+}(z) = 2D^{\pi+}(z) \tag{14}$$

Comparing this with eq. (13) we immediately obtain the simple relationship:[6]

$$\left(\frac{1}{\sigma}\frac{d\sigma^{\pi^+}}{dz}\right)_{e^+e^-} = 2\left(\frac{1}{\sigma}\frac{d\sigma^{\pi^+}}{dz}\right)_{ep} \qquad (z \ \ \text{small}) \tag{15}$$

On the other hand, in the large z region ($z > 1/2$, say), we expect to be able to describe the pion as a symmetrized state of 1 up-quark with 1 down-antiquark, so that $D_u^{\pi+}(z) \approx D_{\bar{d}}^{\pi+}(z)$ with all other $D_i^{\pi+} \simeq 0$. In this case we end up with

$$\left(\frac{1}{\sigma} \frac{d\sigma^{\pi^+}}{dz} \right)_{e^+e^-} \simeq \frac{15}{16} \left(\frac{1}{\sigma} \frac{d\sigma}{dz}\right)_{ep} \qquad (z \text{ large}) \tag{16}$$

The origin of the factor 2 in eq. (15) is easy to understand: the crucial difference between production in e^+e^- and ep processes is that in the former there are two quark lines in the final state which can fragment to produce a pion whereas in the latter case there is only one. If the D_i are all equal as presumably they are when z is small, then the factor 2 follows trivially. The reduction to the factor 15/16 in the large z region, as given in eq. (16), depends upon the details of the weightings given the various quarks in that region. Although these results should not be taken too seriously, they at least indicate rough orders of magnitude to be expected from the one particle spectra based on this model. Figure 2 shows an estimate of the π^+-distribution based on fits of the D's from electroproduction data.[7]

It should be noted that the small z region is sensitive to two effects which we have not taken into account and which could be the origin of an apparent scale-breaking. The first is the effect of a finite transverse momentum cut-off p_T ($\sim \frac{1}{2}$ GeV) which has been neglected throughout this discussion. Our results, and in particular the scaling of $f^{\pi}(z)$, can be expected to be valid only for $z \gg 2p_T/\sqrt{s}$; for example, for $\sqrt{s} \approx 4$ GeV, we need $z \gg .25$. The other point we wish to emphasize is that effects due to a finite m_Q in the dynamical calculation can induce interesting effects in the single particle distribution $s\frac{d\sigma}{dz}$. This is expected to scale for structureless quarks. As an example, imagine an expansion of the form (7) and (8) for the analogs here of W_1 and νW_2. In that case the structure of the single particle distribution takes the form

$$s\,\frac{d\sigma}{dz} \sim G^2(s)\ [(A + \frac{1}{2}\,\mu_Q^2 s)\ \mathscr{F}(z) + \mu_Q^2 m_Q^2\ \mathscr{G}(z)] \tag{17}$$

where A is a constant (~ 1), $\mathscr{F}(z)$ is a scaling function which is a combination of the $D_i(z)$, and $\mathscr{G}(z)$ is related to their approach to scaling; this equation is basically analogous to eq. (9). Now it is not difficult to show that if $\mathscr{F}(z) \to (1-z)^{n+1}$ as $z \to 1$ then $\mathscr{G}(z) \to (1-z)^n$ <u>or slower</u>. Hence, for $z \to 1$ we expect

$$s\,\frac{d\sigma}{dz} \propto G^2(s)(1-z)^n\ [(A + \frac{1}{2}\,\mu_Q^2 s)(1-z) + \beta m_Q^2 \mu_Q^2] \tag{18}$$

where β is some constant. Hence we expect the scale-breaking effects in $s\,\frac{d\sigma}{dz}$ to be enhanced for small z and relatively suppressed for large z. However, if we consider $f^\pi(z) = (1/\sigma)\ (d\sigma^\pi/dz)$ such scale-breaking effects are cancelled out:

$$f^\pi(z) \equiv \frac{1}{\sigma}\ \frac{d\sigma^\pi}{dz} \sim \mathscr{F}(z) + \frac{\mu_Q^2 m_Q^2}{A + \frac{1}{2}\,\mu_Q^2 s}\ \ \mathscr{G}(z) \tag{19}$$

so $f^\pi(z)$ should scale in this model. On the other hand, its approach to scaling should be somewhat slower for small z than for large z because of the different threshold behaviors of $\mathscr{G}(z)$ and $\mathscr{F}(z)$. We thus see that both this and the finite p_T effect produce rather similar effects; namely, to delay the onset of scaling for small z relative to large z. In this regard we note that since multiplicities are essentially determined by the behavior of the distribution functions at small z we cannot make reliable predictions in the energy range of the present experiments. The present model cannot thus account for the apparent rise in the ratio of the energy carried by neutrals to that carried off by charged particles since we are unable to describe the production when low momentum particles are detected. An important test of these ideas would be to measure a quantity like the mean square energy of the secondaries which tends to emphasize the large z region:

$$\begin{aligned}\langle E_\pi^2\rangle &\equiv \int_0^1 dz\, E_\pi^2 \frac{1}{\sigma} \frac{d\sigma^\pi}{dz} \\ &= \frac{s}{4} \frac{\int_0^1 dz\, z^2 \sum e_i^2 D_i^\pi(z)}{\sum e_i^2} \\ &\propto s\end{aligned} \tag{20}$$

Should this prove to be wrong, then the naive model even with structure is indeed in serious trouble.

Finally, we wish to make some remarks concerning the angular distribution of the fast-moving secondaries. This can be described by the function:

$$N(s,\theta) = 1 + \left(\frac{1 - \mu_Q^2 s}{1 + \mu_Q^2 s}\right) \cos^2\theta + O(m_Q^2, \mu_Q m_Q) \tag{21}$$

For small values of s this reproduces the familiar $(1 + \cos^2\theta)$ distribution characteristic of Bhabha scattering. However, as s grows, the distribution should become more and more isotropic reaching perfect isotropy at $s = \mu_Q^{-2} \simeq 50\ \mathrm{GeV}^2$. Beyond this, the distribution approaches a $\sin^2\theta$ configuration (see fig. 3). Obviously, these remarks are modified by the finite p_T effect which we have not taken into account and which is presumably most important for small s where it tends to distort the $(1 + \cos^2 \theta)$ behavior into a more isotropic configuration. It is worth pointing out that $N(s,\theta)$ approaches isotropy rather rapidly yielding approximate isotropy even for $s \sim \frac{1}{2} \mu_Q^{-2} \sim 25 \text{ GeV}^2$.

c) Neutrino and Anti-Neutrino Scattering

In order to reduce the large number of possible parameters that could enter into the description of the quark matrix element of the conventional weak charged current, we make several simplifying assumptions, some of which are motivated from a physical standpoint others from a technical one. These are as follows: (i) charmed quarks are not excited; (ii) the CVC hypothesis is valid; (iii) the Cabbibo angle is zero; (iv) the axial vector form factors have a similar shape to the vector ones and (v) effects due to a possible heavy intermediate vector boson (W) are neglected (such effects cannot be distinguished from those of a form factor). We shall not discuss effects which amend the presence of neutral weak currents but shall have some words concerning the presence of second class currents. With the above assumption we can write the vertex for the weak transition of a u-quark to a d-quark as:

$$G(q^2)\ \tau_+\{\gamma_\nu(1-\lambda\gamma_5) - \mu_Q(p + p')_\nu\} + O(m_Q^2,\ \mu_Q m_Q) \qquad (22)$$

where τ_+ is quark isospin raising operator and λ the renormalized value of the quark axial vector coupling constant (the analog of G_A) and is thus expected to be ~ 1 (indeed on dimensional grounds one might expect its deviation from 1 to be $O(\mu_Q m_Q)$). The calculation of the neutrino and antineutrino cross-sections proceeds in an identical way to that of the electromagnetic structure functions. We shall employ the conventional variables as before: q is the four-momentum transferred by the leptons to the target, ν the corresponding energy in the laboratory system, and $x = -q^2/2\nu M$; we shall also use $y = \nu/E$ and[8] $v = xy = -q^2/2ME$, E being the incident energy. With these definitions we find for the neutrino and antineutrino cross sections:

$$\frac{d^2\sigma}{dx\ dy} = \frac{2G^2ME}{\pi} \frac{x}{[1 + 2MExy/\Lambda^2]^2} \{f\ q(x) + \bar{f}\ \bar{q}(x)\} \tag{23}$$

$$\frac{d^2\bar{\sigma}}{dx\ dy} = \frac{2G^2ME}{\pi} \frac{x}{[1 + 2MExy/\Lambda^2]^2} \{\bar{f}\ q(x) + f\bar{q}(x)\} \tag{24}$$

where $q(x) = [u(x) + d(x)]/2$ and the bar indicates that a charge conjugation is implied. The functions f and $\bar{f}$ are given by:

$$f = \left(\frac{1+\lambda}{2}\right)^2 + \left(\frac{1-\lambda}{2}\right)^2 (1-y)^2 + \mu_Q^2\ ME\ xy(1-y) \tag{25}$$

$$\bar{f} = \left(\frac{1+\lambda}{2}\right)^2 + (1-y)^2 + \left(\frac{1-\lambda}{2}\right)^2 + \mu_Q^2\ ME\ xy(1-y) \tag{26}$$

Note that when $\lambda = 1$ and $\mu_Q = 0$ these reduce to $f = 1$ and $\bar{f} = (1-y)^2$, respectively, which correspond to the conventional quark-parton model results. As already intimated we do not expect λ to deviate from 1 by very much (certainly $\lesssim 20\%$, say) in which case we can effectively neglect the $(1 - \lambda)^2/4$ terms. In that case, the $(1 + \lambda)^2/4$ terms only change the absolute normalization of the cross-sections in an energy independent fashion (inducing an apparent effective value of $\mu_Q \to 2\mu_Q/(1+\lambda)$). In our numerical calculations we have therefore set $\lambda = 1$; different λ values can be obtained by multiplying by $(1+\lambda)^2/4$. It is worth pointing out in this regard that if charge symmetry were violated then μ_Q occurring in eq. (22) may not be identical to the anomolous moment used in eq. (1). Furthermore, should there be a piece of a second class current present, parametrized as $\mu_{5Q}\,\gamma_5(p + p')_\nu$, its effect here only changes $\mu_Q^2 \to \mu_Q^2 + \mu_{5Q}^2$. Some immediate consequences of our model (up to obvious corrections on the quark level) are clear:

i) The ratio $(d^2\bar{\sigma}/dx\,dy)/(d^2\sigma/dx\,dy)$ is independent of Λ and is sensitive only to μ_Q much as σ_L/σ_T is in the electromagnetic case. Since as $x \to 0$, we expect $q(x) \sim \bar{q}(x)$, this ratio approaches 1 (independent of y) as in the usual model. However, away from $x \simeq 0$ (e.g., $x \gtrsim .2$) we expect $\bar{q}(x) \simeq 0$, in which case this ratio approaches $\bar{f}/f$, i.e.,

$$\frac{d^2\bar{\sigma}/dx\,dy}{d^2\sigma/dx\,dy} \xrightarrow{x \gtrsim .2} \frac{(1-y)^2 - \frac{1}{2}\mu_Q^2\, q^2(1-y)}{1 - \frac{1}{2}\mu_Q^2\, q^2(1-y)} \tag{27}$$

$$\to 1 \quad \text{(independent of } x \text{ and } y\text{)}$$

when $-(1-y)q^2 \gg 2\mu_Q^{-2} \sim 50\ \mathrm{GeV}^2$. In the conventional model without structure this ratio should behave like $(1-y)^2$ in this region. Notice that W propagator effects do not influence the ratio (27). The dependence on μ_Q can be eliminated by considering the difference $(d^2\sigma/dx\,dy)-(d^2\bar{\sigma}/dx\,dy)$ which is sensitive only to Λ:

$$\frac{d^2}{dx\,dy}(\sigma - \bar{\sigma}) = \frac{2G^2ME}{\pi}\,\frac{xy(2-y)}{[1 + 2ME\,xy/\Lambda^2]^2}\,\{q(x) - \bar{q}(x)\} \tag{28}$$

which differs from the usual form only by the presence of the form factor.

ii) As in the electromagnetic case the presence of μ_Q tends to diminish the effects of the finite quark radius. Here, however, because we are expressing our results directly in terms of a cross-section rather than in terms of structure functions, the delicate cancellation which maintained apparent scaling in the νW_2 does not maintain scaling for the cross-sections. The point is that the cross-section involve the analogs of νW_2 and W_1 (as well as the axial and vector interference structure function W_3) but, as we saw, scaling is broken relatively badly in W_1 (reflected in the predicted growth of σ_L/σ_T with $-q^2$) so in the measured cross-section, scaling should, at measurable energies, eventually be badly broken. Such an effect is expected to show up more readily in the neutrino interactions because these are not heavily damped by the photon propagator appearing in the electromagnetic case which, up to now, has predominently allowed for a sensitive measurement of W_2 only.

iii) The structure effects tend to be considerably larger in neutrino than in antineutrino scattering. As an example of this, suppose we are away from the diffractive region ($x \sim 0$) so that we can neglect $\bar{q}(x)$ relative to $q(x)$ then for $-q^2 \ll \Lambda^2$ we can expand the form factor and express eqs. (23) and (24) in the approximate form

$$\frac{d^2\sigma}{dx\ dy} \simeq \frac{2G^2ME}{\pi} xq(x) \left[1 - (1+y)\ \mu_Q^2 ME\ xy\right] \tag{29}$$

$$\frac{d^2\bar{\sigma}}{dx\ dy} \simeq \frac{2G^2ME}{\pi} xq(x)\ (1-y)^2 \left[1 - \left(\frac{1-2y}{1-y}\right) \mu_Q^2 ME\ xy\right] . \tag{30}$$

In writing these equations we have set $2/\Lambda^2 \approx \mu_Q^2$ which is an approximate condition required to maintain the observed scaling in νW_2. For neutrino scattering the extra factor $(1+y)\ \mu_Q^2\ ME\ xy$ is always positive thus always depressing the cross-section. On the other hand, for antineutrino scattering the extra factor $(1-2y/1-y)\ \mu_Q^2 ME\ xy$ changes sign at $y = 1/2$ and can therefore add or subtract from the cross-section. Furthermore, whereas $1 \leq 1+y \leq 2$ for the complete kinematic range, $|(1-2y)/(1-y)| \leq 1$ for $0 < y < 2/3$; for $y > 2/3$ this antineutrino factor becomes very large, however its effect there is quite unimportant because of the presence of the overall $(1-y)^2$ factor in the cross-section. We thus see that, indeed, the form factor and magnetic moment effects tend to oppose each other in antineutrino cross-sections (much as they do in the e^+e^- case). It is clear then that a characteristic signal for the presence of quark structure is a significant deviation in scaling in the neutrino cross-section but only a small (or perhaps no) effect in the antineutrino one. Put slightly differently, we can expect ratios of neutrino to antineutrino cross-sections to be enhanced over the simple model predictions.

Because of limited statistics in the foreseeable future, it is unlikely that experiments will be able to give reliable detailed analysis of the cross-sections af functions of the three variable x, y and E.

When making numerical estimates, we have therefore turned our attention to one-parameter distributions and to the total cross-sections themselves which can be more easily explored experimentally. Furthermore, we have selected distributions which tend to be rather insensitive to a detailed knowledge of the quark distribution functions $q(x)$ and $\bar{q}(x)$: thus a convenient parameterization of these functions, such as that given by Barger and Phillips,[9,10] should be sufficiently accurate as long as one does not consider quantities which are sensitive to the $\bar{q}$ content of the nucleon. We have also extended the simple pole parametrization of the form factor out to values of $-q^2 \sim 200\ \mathrm{GeV}^2$ which is hardly justifiable. Our results and predictions should therefore be considered with that in mind. Our numerical calculations are shown in figs. 4-9. In each of these we have presented (i) the scaling predictions without structure; (ii) the predictions including only a form factor; (iii) predictions including the full effects of structure, i.e., both a form factor and an anomalous magnetic moment; and (iv) we have indicated the effects due to the presence of second class currents. Although most of the features of these graphs are self-explanatory, some comments are worth emphasizing.

a) For the total cross-sections (figs. 4) we see that the effect of structure is considerable in neutrinos (especially at high energies) whereas it is considerably less in antineutrinos, consistent with our previous remarks following eqs. (23) and (24). In fact, by increasing μ_Q^2 (or, alternatively, introducing a finite value of $\mu_{5Q}^2 \sim \mu_Q^2$, coming from second class currents) we could eliminate or even reverse the direction of the scale-breaking in $\bar{\sigma}$. In fig. 5 we have plotted the ratio $\bar{\sigma}/\sigma$ which, in the structureless case, is constant ($\sim 1/3$) independent of E.

As expected, structure induces a significant rise in this ratio, its magnitude being rather sensitive to μ_Q and Λ (and therefore the shape of the form factor) as well as the antiquark distributions $\bar{q}(x)$ which are not well-known. The size should therefore not be taken too seriously; nevertheless, some significant and observable rise should be seen if these ideas are correct.

b) In figs. 6 and 7 we show the mean values of $v = xy$ and y as functions of E. Since both of these de-emphasize the $y \sim 0$ region we can expect them to show even less scale breaking in the antineutrino case than in the total cross-section $\bar{\sigma}$. This is indeed the case, especially in $\langle xy \rangle$, which also suppresses the $x \sim 0$ region; note that we have normalized this distribution to the total-cross-section in order to remove any unnecessary beam energy dependence which may not be well determined; (v is determined by measuring the energy and scattering angle of the outgoing lepton only[8]).

Figure 8 shows v-distributions, at an incident energy of 150 GeV. Remarks similar to the above can be made here. Empirically, these curves can be well approximated in the region of interest $.05 \leq v \leq .5$ by an exponential of the form

$$\frac{1}{\sigma}\frac{d\sigma}{dv} = e^{A-Bv} \quad . \tag{31}$$

If the cross-section scales then A and B are energy independent, the slope parameter B is most sensitive to finite size effects. In Table I we have presented values of A and B for various parameters and energies $E = 50$ GeV and $E = 150$ GeV, in order to give some idea of their dependencies.

d) Figure 9 shows the y-distributions $d\sigma/dy$ and $d\bar{\sigma}/dy$ again for an incident energy of 150 GeV. As $y \to 1$, the effects due to the anomalous moment vanish, leaving only an effect of the radius. Again, scaling deviations in $d\bar{\sigma}/dy$ are very small whereas in $d\sigma/dy$ they are extremely large. This startling result incidentally is independent of the number of anti-quarks in the nucleon.

III. CONCLUSIONS

In this paper we have examined some of the experimental consequences of quark structure which can be tested in the near future. Our starting point was the observation that, within the context of the conventional impulse approximation, the dominant effect of quark structure at presently available energies is to give the quark a size (i.e., a form factor) as well as an anomalous magnetic moment. We have previously shown[4] that these can be arranged in such a way that the observed scaling phenomenon in deep inelastic electron scattering can still be preserved whilst, at the same time, the observed rise in the ratio $\sigma(e^+e^- \to \text{all hadrons})/\sigma(e^+e^- \to \mu^+\mu^-)$ can be achieved. Some of the new and more striking experimental consequences of this model can be summarized as follows:

a) An eventual rise in the ratio σ_L/σ_T should be seen reflecting a significant scale violation in W_1 for $-q^2 \gtrsim 20\ \text{GeV}^2$ (see eq. (6)).

b) For $z \gtrsim .2$, the single particle distribution function for the detection of one pion in e^+e^- scattering $((1/\sigma)/(d\sigma^\pi/dz))$, should violate scaling mostly in the regions of smaller z. (See eq. (18).)

The angular distribution of the fast-moving secondaries should be almost isotropic; see eq. (21).

c) There should be large scale-breaking effects in neutrino-scattering whereas, for antineutrinos, such effects should be quite small.

Should future experiments indicate the validity of these predictions, then indeed the idea of quark structure and all its ramifications would have to be seriously considered. Some of these are already to be found in refs. 2. On the other hand, should there be striking disagreement with any of these predictions, then it is unlikely that the model should be considered much further.

In the event that experimental data forces a further substructure upon us, it is useful to anticipate other places to look for its consequences. Some of these might be the following:

a) Polarization experiments:[12] all the experiments considered in this paper deal with unpolarized cross-sections in which the interference between electric and magnetic scattering averages to zero so that the effects of the anomolous moment come in quadratically ($\propto \mu_Q^2$), which is small. However, in polarized experiments it is possible, in principle, to see effects linear in μ_Q; although such experiments are very difficult, the effects should be quite striking, since on dimensional grounds they should be of order $(\mu_Q/m_Q)q^2 \sim \frac{2}{3}\, q^2$!!

b) The production of $\mu^+\mu^-$ pairs in proton-proton collision, $pp \rightarrow \mu^+\mu^-$ + anything, has been investigated by Drell and Yan[13] within the conventional parton model. They showed that one expects $q^4\, d\sigma/dq^2$ to scale to a function of $\tau = s/q^2$ only, where $\sqrt{q^2}$ is the invariant mass of the $\mu^+\mu^-$ pair and $\sqrt{s}$ is the initial center of mass energy of the process. Such an experiment has been performed[14] and found to indicate serious violations of the model predictions. In particular, the calculation suggests a smooth distribution in τ whereas the data shows a significant bump for τ values near ~ 0.2. Since there are several difficulties in the interpretation of this experiment, such a result should not be taken too seriously at this stage. Nevertheless, within the context of our model the Drell-Yan prediction must be modified by a factor like $(1 + \frac{1}{2}\mu_Q^2 s\tau)/(1 - s\tau/\Lambda^2)^2$ and it is amusing to consider its consequence. If it is indeed correct then it says that there is in fact an energy-dependent bump in the τ distribution for large s values arising from the growth of the form factor in this region analogous to the growth in $\sigma_{e^+e^-}$. Whether this is the origin of the bump seen in the experiment is not clear, especially since there are phase-space effects to be taken into account because of the finite values of s involved. As an attempt along these lines we have factored out the above factor from the data to see if the remainder is smooth. Unfortunately, remnants of the bump still remain and we will have to await future experiments at higher values of s to see if it is indeed real.

Finally, we should emphasize that all of the structure effects discussed in this paper represent only a transition region; eventually gluons are produced and a new region opens up. What happens in this region is far from clear; it may be, for example, that at energies well above gluon production threshold, the "bareness" of spin 1/2 quarks is completely created and scaling again sets in with $\sigma_L/\sigma_T \to 0$. In a model where the conventional Gell-Mann-Zweig quarks are "bound states" of Han-Nambu quarks and gluons, the vector gluon carries charge so above production scaling may be changed and the ratio σ_L/σ_T most probably will not approach zero. In any case, we could be assured of a new regime of physics!

ACKNOWLEDGMENTS:

We would like to thank J. D. Bjorken, M. S. Chanowitz, and F. J. Gilman for useful discussions and M.-S. Chen for helping with the numerical calculations. One of us (P.Z.) expresses his gratitude to S.D. Drell for the warm hospitality extended to him at SLAC.

TABLE I

EXPANSION COEFFICIENTS IN $\frac{1}{\sigma}\frac{d\sigma}{dv} = e^{A-Bv}$ for $.05 \lesssim v \lesssim .5$.

	$A(\nu)$		$B(\nu)$		$A(\bar{\nu})$		$B(\bar{\nu})$	
	E = 50	E = 150	E = 50	E = 150	E = 50	E = 150	E = 50	E = 150
$\mu_Q^2 = 0$, $\Lambda^2 = \infty$	1.90		6.67		2.40		12.8	
$\mu_Q^2 = .02$, $\Lambda^2 = 100$	1.90	2.24	6.61	9.78	2.16	2.23	10.3	11.9
$\mu_Q^2 = 0$, $\Lambda^2 = 100$	2.08	2.22	8.18	10.0	2.48	2.49	14.3	16.0
$\mu_Q^2 = .02$, $\Lambda^2 = \infty$	2.09	1.90	8.11	6.50	2.26	2.04	11.8	8.65

REFERENCES

1. R. P. Feynman, Photon-Hadron Interactions, W. A. Benjamin, Inc., 1972.
   J. D. Bjorken and E. A. Paschos, Phys. Rev. 185, 1975 (1969) and Phys. Rev. D1, 3151 (1970).
2. M. Chanowitz and S. D. Drell, Phys. Rev. Letters 30, 807 (1973) and SLAC-Pub. 1315.
3. A. Litke et al., Phys. Rev. Letters 30, 1189 (1973).
   B. Richter, Talk presented to the Irvine Conference, Dec. 1973.
4. G. B. West, Stanford University preprint, Jan. 1974.
5. E. D. Bloom, Talk presented to the International Symposium on Electron and Photon Interactions at High Energies, Bonn 1973.
6. A comparison of experimental data along this line has been carried out by **G. Feldman.**
7. J. D. Bjorken, Talk presented to the Bonn Conference 1973;
   J. Cleymans and R. Rodenberg, Aachen preprint, Aug. 1973
8. J. D. Bjorken, D. Cline, and A. K. Mann, Phys. Rev. **D8, 3207 (1973).**
9. V. Barger and R.J.N. Phillips, Wisconsin University preprint, 1973.
10. Finite size effects have been discussed by V. Barger, Wisconsin University preprint, 1973.
11. B. C. Barish et al., Phys. Rev. Letters 31, 565 (1973);
    A. Benvenŭti et al., Phys. Rev. Letters 31, 1018 (1973);
    A. Benvenŭti et al., Phys. Rev. Letters 32, 125 (1974).
12. **E. W. Colglazier and R. Rajarman, Princeton preprint, 1974.**
13. S. D. Drell and T.-M. Yan, Phys. Rev. Letters 25, 316 (1970).
14. J. H. Christenson et al., Phys. Rev. D4, 2016 (1973).

CAPTIONS

Figure 1. Ratio of longitudinal to transverse cross section in electron-proton scattering; anomalous moment of the quarks is assumed to be $\mu_Q^2 = .02\ \mathrm{GeV}^{-2}$. Data from Ref. 5.

Figure 2. Estimate of π^+-distribution in e^+e^- annihilation within the quark model. Quark fragmentation functions $D_u^{\pi^+}$ and $D_d^{\pi^+}$ are taken from fits of electroproduction data by Bjorken (curve (a)) and Cleymans and Rodenberg (curve (b))[7]; all other D_i's are put equal to $D_d^{\pi^+}$.

Figure 3. Polar diagram for the angle distribution of secondaries in a structured quark model (with vanishing p_T).

Figure 4. Total neutrino and antineutrino-nucleon (I = 0) cross sections as functions of the energy of the ingoing lepton in the laboratory frame. Data from Refs. 11.

Figure 5. Ratio of the total antineutrino to neutrino cross section. Data from Refs. 11.

Figure 6. Average value of $v = xy$ as a function of (anti) neutrino energy. Data are rough estimates from Refs. 11.

Figure 7. Expectation value of the lepton energy loss y; it is <u>not</u> normalized by the cross section in order to emphasize the difference between the models.

Figure 8. Distributions of the relative momentum transfer v for (anti) neutrino energy $E = 150$ GeV. Going back to $E = 50$ GeV diminishes the deviations from the scaling curves by about a factor of 2. The parameters of the nearly exponentially decreasing functions are summarized in the Table for both energies.

Figure 9. Distributions of the energy loss y for $E = 150$ GeV.

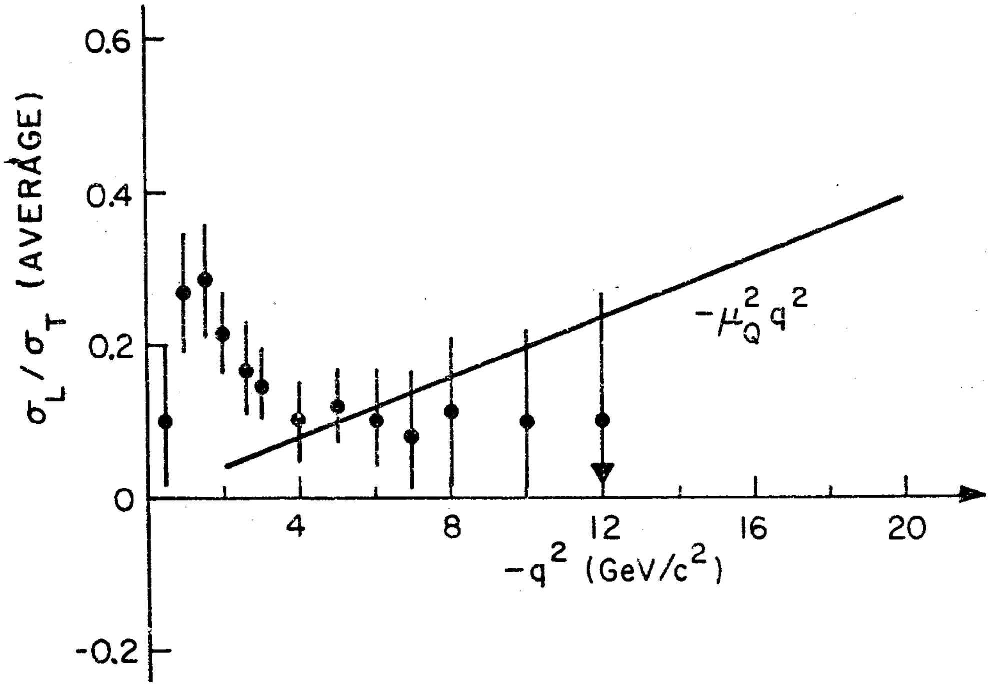

0.6
0.4
0.2
0
-0.2
σ_L/σ_T (AVERAGE)
$-\mu_Q^2 q^2$
4
8
12
16
20
$-q^2$ (GeV/c^2)

Fig. 1

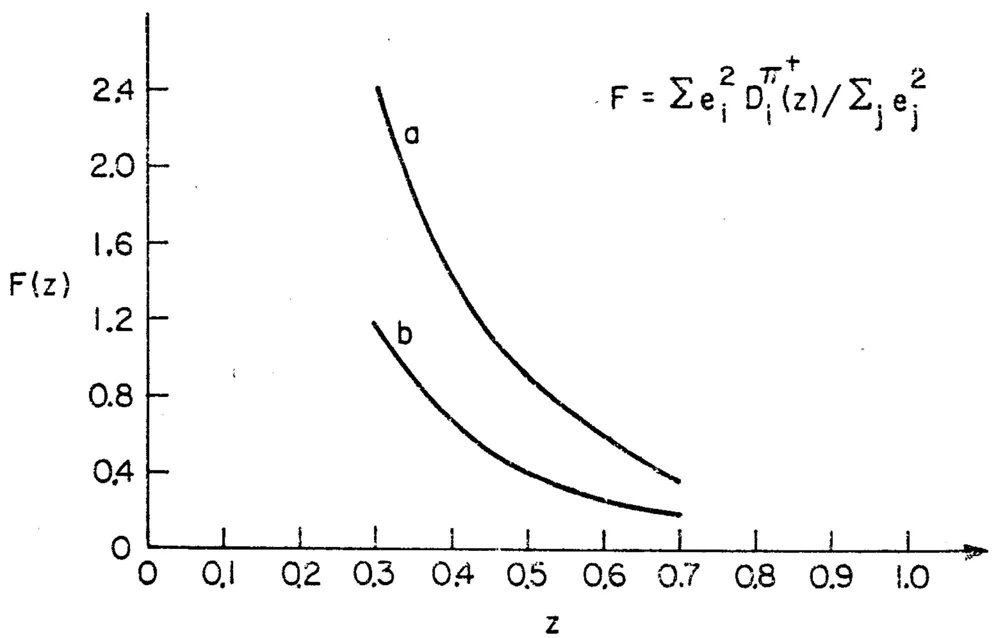

$F = \Sigma e_i^2 D_i^{\pi^+}(z)/\Sigma_j e_j^2$
2.4
2.0
1.6
1.2
0.8
0.4
0
F(z)
a
b
0
0.1
0.2
0.3
0.4
0.5
0.6
0.7
0.8
0.9
1.0
z

Fig. 2

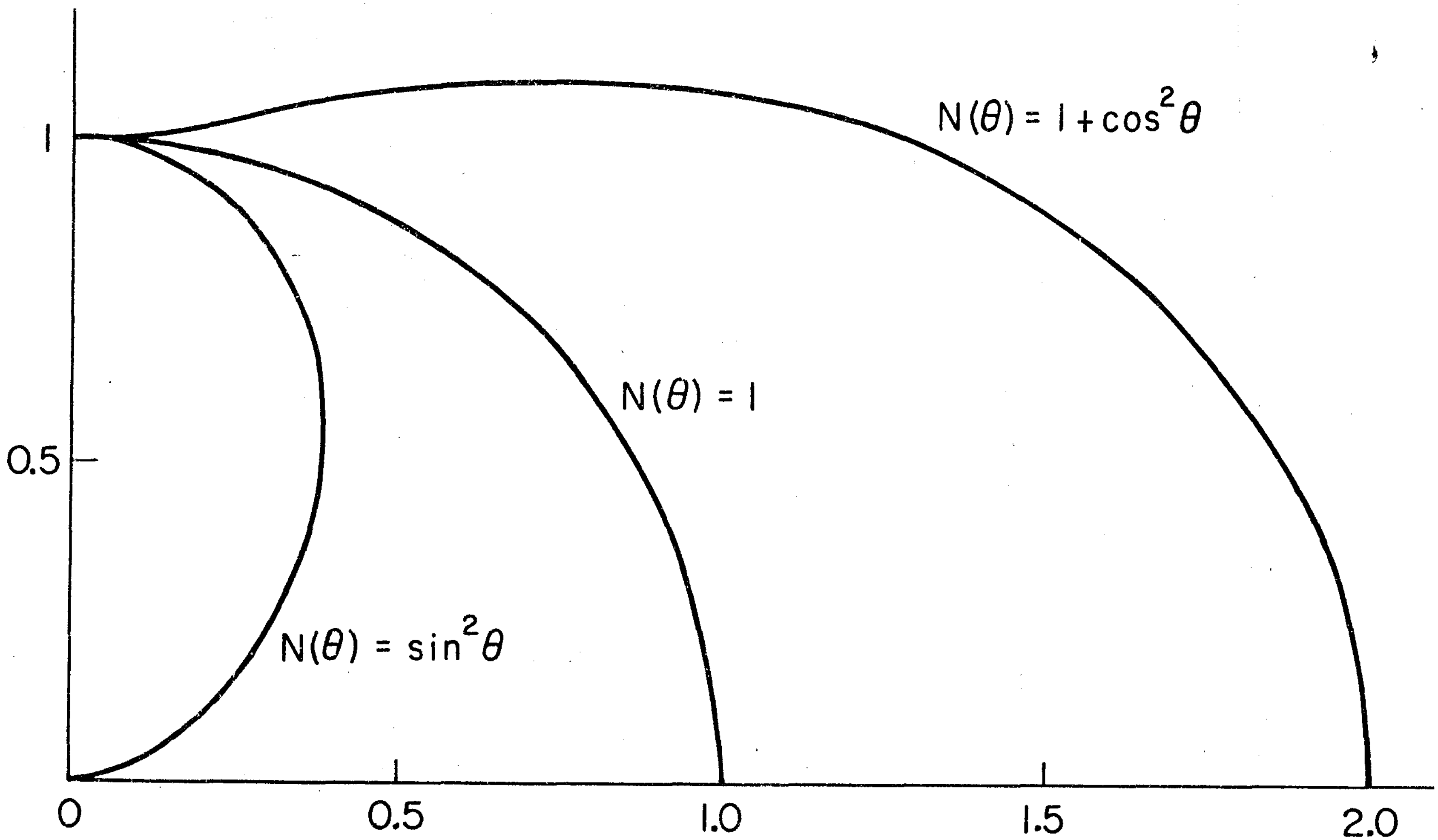

Fig. 3

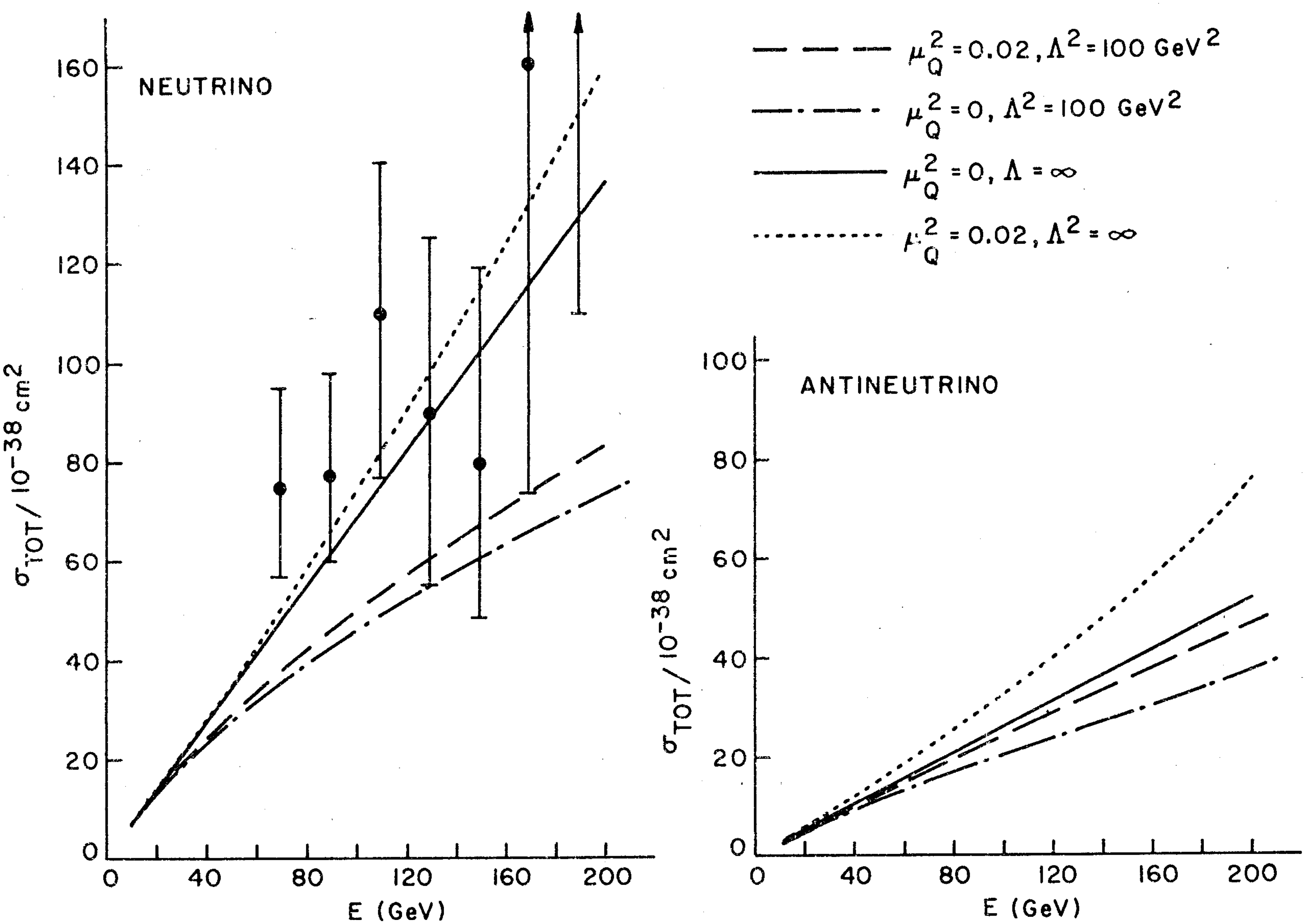

$\mu_Q^2 = 0.02,\ \Lambda^2 = 100\ \mathrm{GeV}^2$
$\mu_Q^2 = 0,\ \Lambda^2 = 100\ \mathrm{GeV}^2$
$\mu_Q^2 = 0,\ \Lambda = \infty$
$\mu_Q^2 = 0.02,\ \Lambda^2 = \infty$
NEUTRINO
ANTINEUTRINO
$\sigma_{TOT}/10^{-38}\,\mathrm{cm}^2$
E (GeV)

Fig. 4

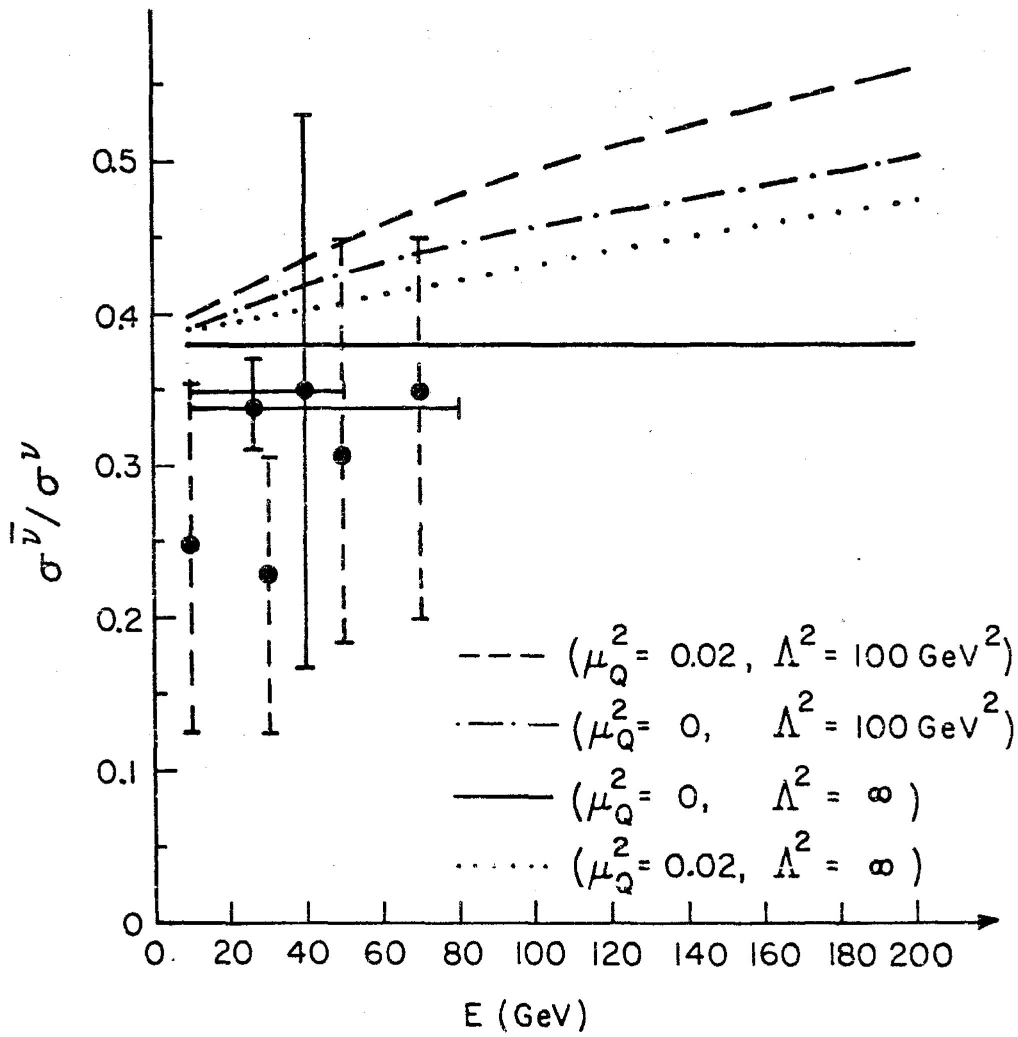
0.5
0.4
0.3
0.2
0.1
0
$\sigma^{\bar{\nu}}/\sigma^{\nu}$
0. 20 40 60 80 100 120 140 160 180 200
E (GeV)
$(\mu_Q^2 = 0.02,\ \Lambda^2 = 100\ \mathrm{GeV}^2)$
$(\mu_Q^2 = 0,\ \Lambda^2 = 100\ \mathrm{GeV}^2)$
$(\mu_Q^2 = 0,\ \Lambda^2 = \infty)$
$(\mu_Q^2 = 0.02,\ \Lambda^2 = \infty)$

Fig. 5

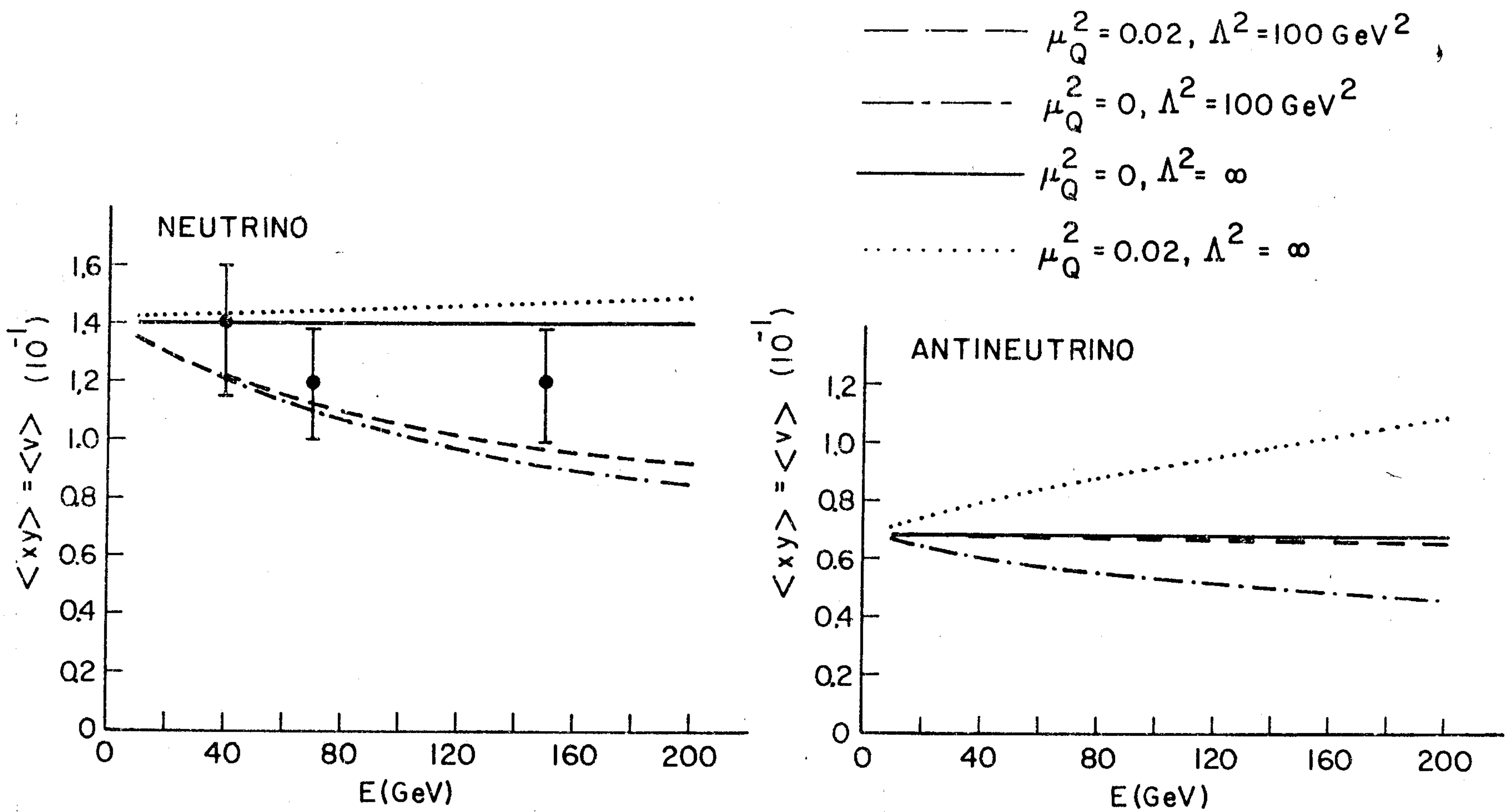

$\mu_Q^2 = 0.02,\ \Lambda^2 = 100\ \mathrm{GeV}^2$
$\mu_Q^2 = 0,\ \Lambda^2 = 100\ \mathrm{GeV}^2$
$\mu_Q^2 = 0,\ \Lambda^2 = \infty$
$\mu_Q^2 = 0.02,\ \Lambda^2 = \infty$
NEUTRINO
ANTINEUTRINO
$\langle xy \rangle = \langle v \rangle \quad (10^{-1})$
E(GeV)
0
40
80
120
160
200
0.2
0.4
0.6
0.8
1.0
1.2
1.4
1.6

Fig. 6

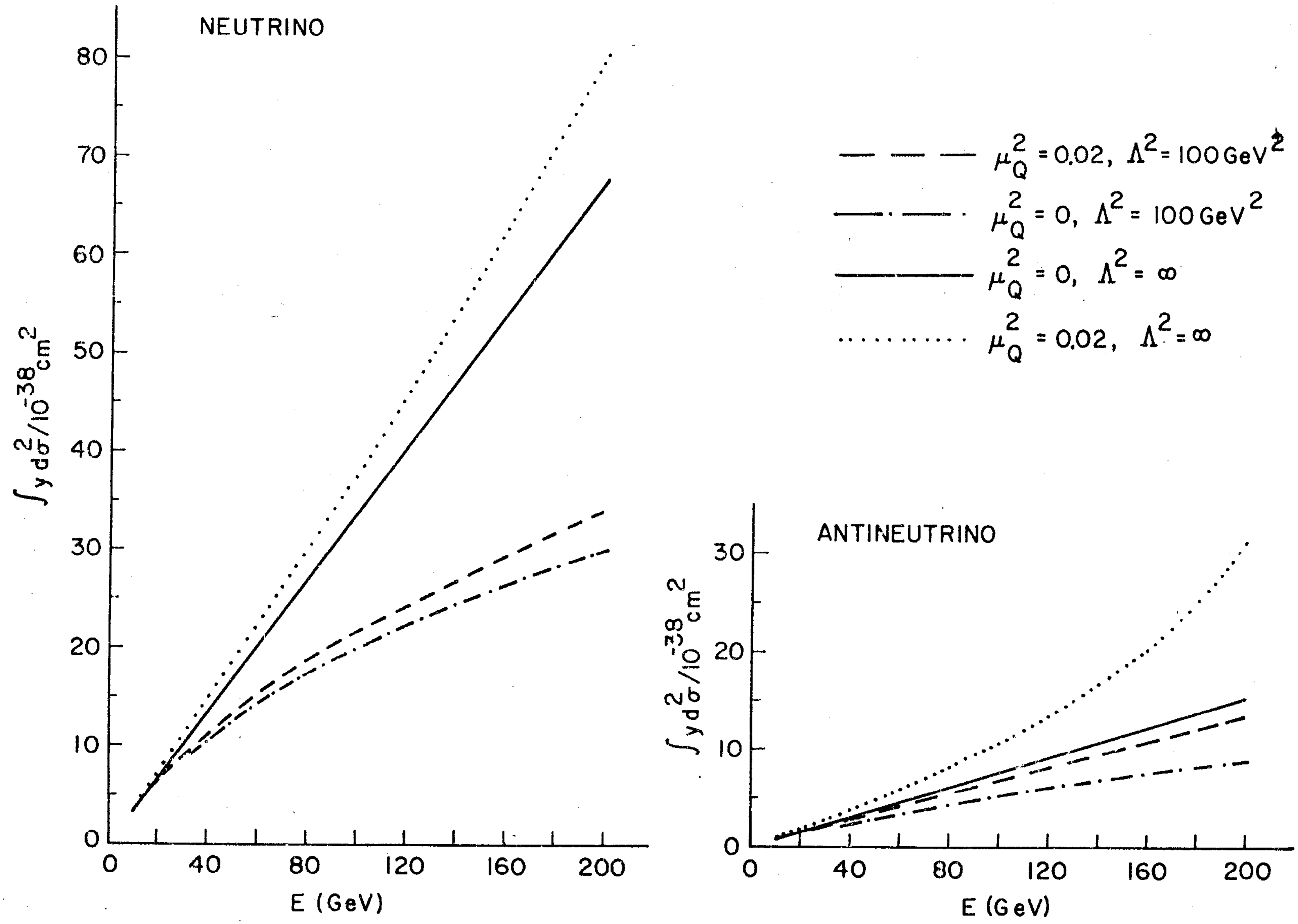
NEUTRINO
ANTINEUTRINO
$\int y\,d\sigma^2/10^{-38}\,cm^2$
E (GeV)
0
10
20
30
40
50
60
70
80
0
40
80
120
160
200
$\mu_Q^2 = 0.02,\ \Lambda^2 = 100\,GeV^2$
$\mu_Q^2 = 0,\ \Lambda^2 = 100\,GeV^2$
$\mu_Q^2 = 0,\ \Lambda^2 = \infty$
$\mu_Q^2 = 0.02,\ \Lambda^2 = \infty$

Fig. 7

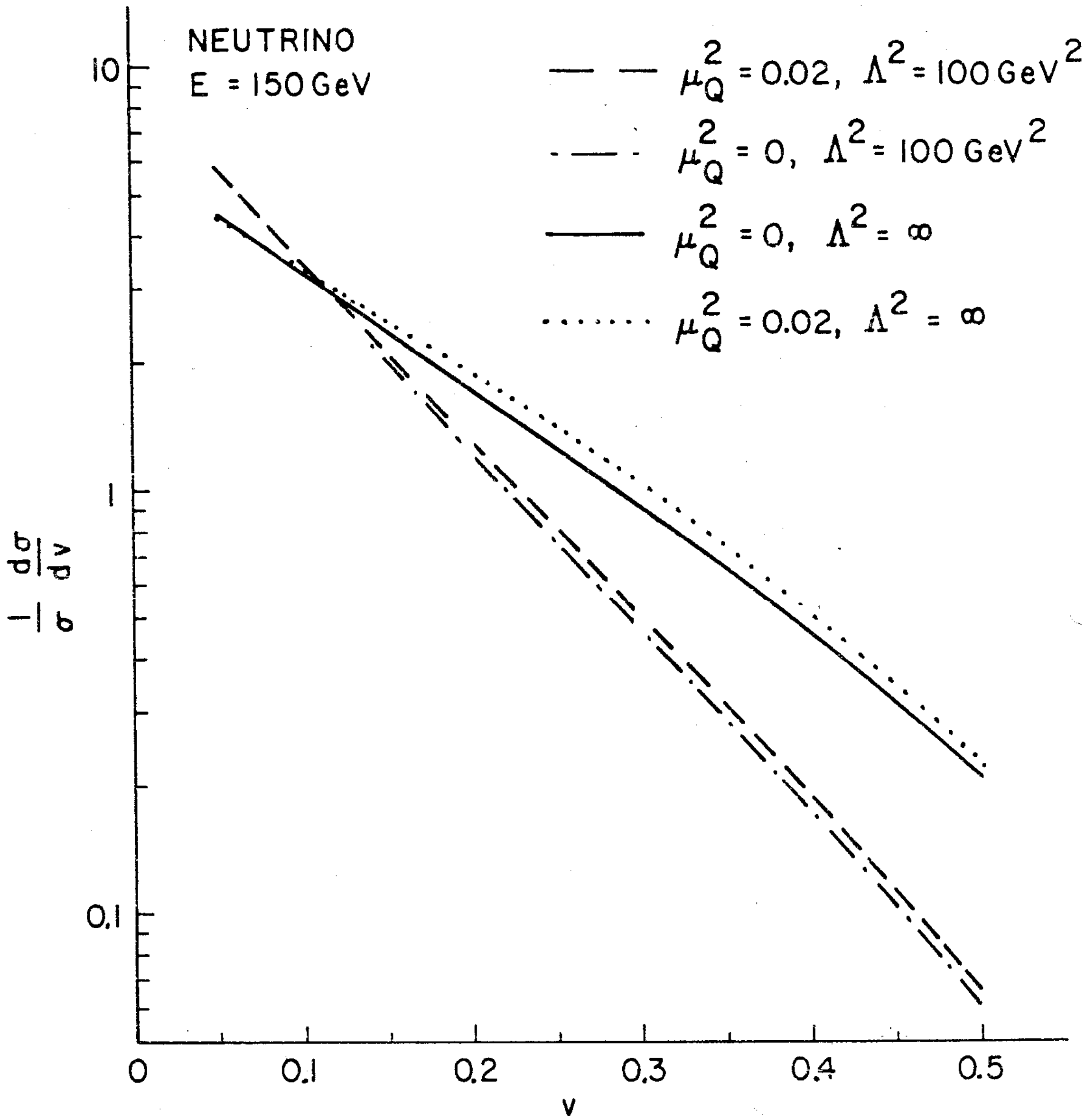
NEUTRINO
E = 150 GeV
$\mu_Q^2 = 0.02,\ \Lambda^2 = 100\,\mathrm{GeV}^2$
$\mu_Q^2 = 0,\ \Lambda^2 = 100\,\mathrm{GeV}^2$
$\mu_Q^2 = 0,\ \Lambda^2 = \infty$
$\mu_Q^2 = 0.02,\ \Lambda^2 = \infty$
10
1
0.1
$\frac{1}{\sigma}\frac{d\sigma}{dv}$
0
0.1
0.2
0.3
0.4
0.5
v

Fig. 8a

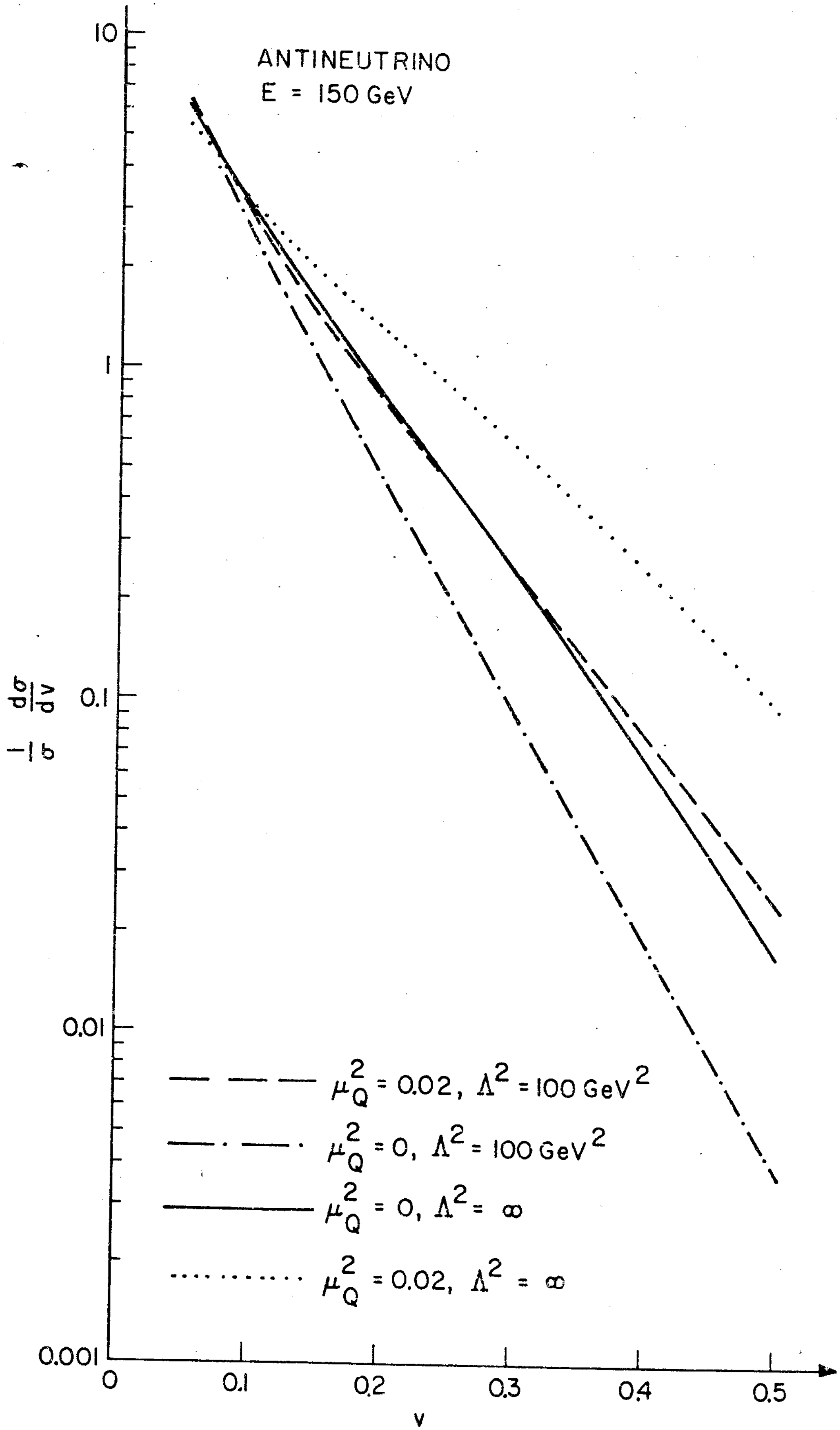
10
1
0.1
0.01
0.001
$\frac{1}{\sigma}\frac{d\sigma}{dv}$
ANTINEUTRINO
E = 150 GeV
$\mu_Q^2 = 0.02,\ \Lambda^2 = 100\ \mathrm{GeV}^2$
$\mu_Q^2 = 0,\ \Lambda^2 = 100\ \mathrm{GeV}^2$
$\mu_Q^2 = 0,\ \Lambda^2 = \infty$
$\mu_Q^2 = 0.02,\ \Lambda^2 = \infty$
0
0.1
0.2
0.3
0.4
0.5
v

Fig. 8b

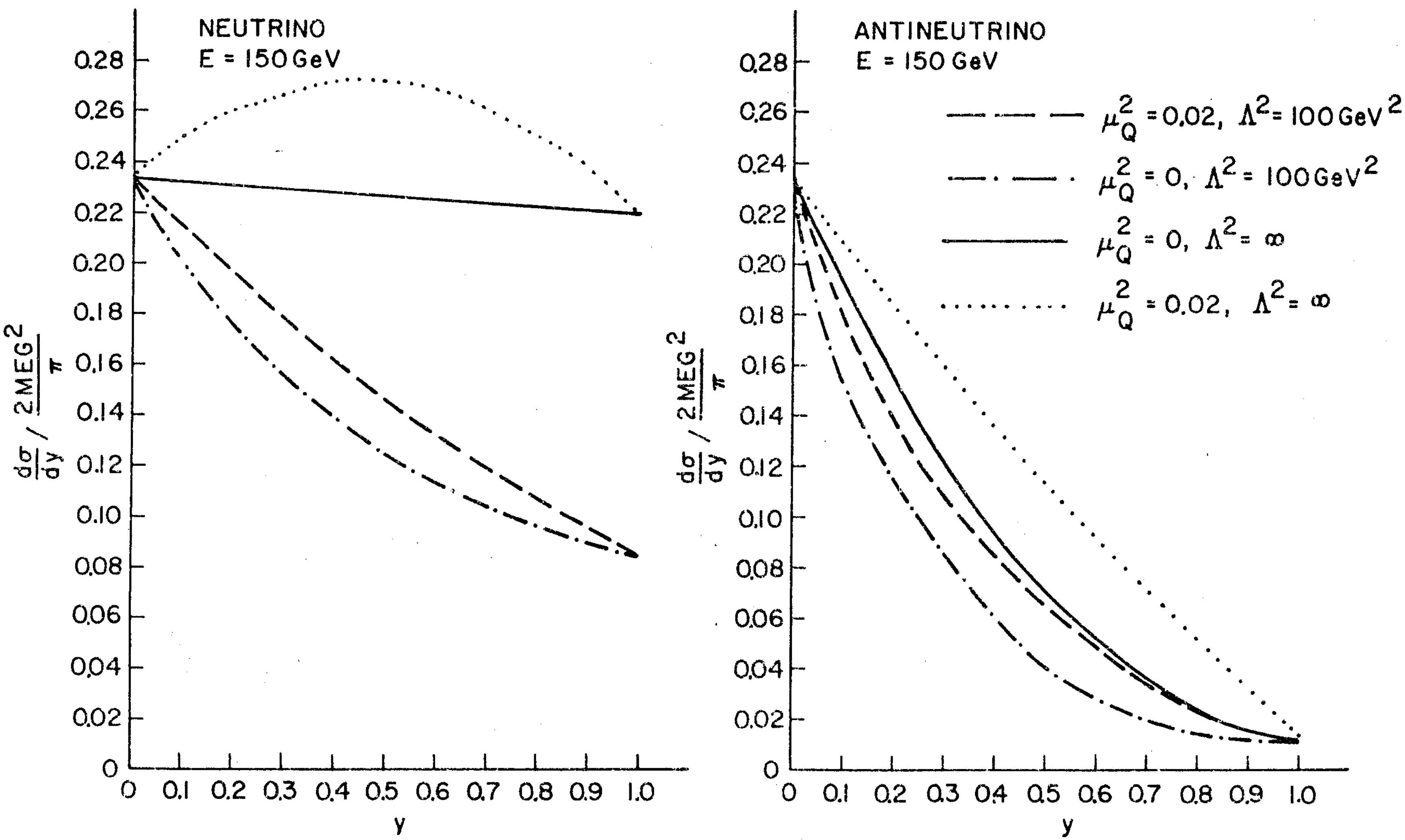
NEUTRINO
E = 150 GeV
ANTINEUTRINO
E = 150 GeV
$\mu_Q^2 = 0.02,\ \Lambda^2 = 100\,\mathrm{GeV}^2$
$\mu_Q^2 = 0,\ \Lambda^2 = 100\,\mathrm{GeV}^2$
$\mu_Q^2 = 0,\ \Lambda^2 = \infty$
$\mu_Q^2 = 0.02,\ \Lambda^2 = \infty$
$\frac{d\sigma}{dy} / \frac{2MEG^2}{\pi}$
y
0.28
0.26
0.24
0.22
0.20
0.18
0.16
0.14
0.12
0.10
0.08
0.06
0.04
0.02
0
0.1
0.2
0.3
0.4
0.5
0.6
0.7
0.8
0.9
1.0

Fig. 9